Central European Journal of Energetic Materials
ISSN 1733-7178; e-ISSN 2353-1843

Cent. Eur. J. Energ. Mater. 2023, *20*(3): 302-317; DOI 10.22211/cejem/168510
Article is available in PDF-format, in colour, at:
https://ipo.lukasiewicz.gov.pl/wydawnictwa/cejem-woluminy/vol-20-nr-3/

Research paper

Study on the Trend in Evolution of the Energy Flow in the Axis of Annular Booster Pellets

Zhong-qing Xue[1,*)], **Jing He**[2)], **Xiong Cao**[3)], **Jun Zhang**[4)]
[1)] *Department of Environmental and Safety Engineering, Taiyan Institute of Technology, Tai Yuan, China*
[2)] *Department of Computer Science, Wuhan Polytechnic, Wuhan, China*
[3)] *Chemical Industry and Ecology College, North University of China, Taiyuan, China*
[4)] *Ordnance Engineering College, Naval University of Engineering, Wuhan, China*
* *E-mail:* xzq2701@163.com

Abstract: In order to further understand the detonation characteristics of annular booster pellets, the energy convergence effect from the detonation wave on the central axis was investigated by using the segmentation and lower end surface output. The result shows that in the whole explosion process, the power exportation capability (N) of the converging energy flow into the central axis increases, then decreases, and then increases and finally decreases. When the collision incidence angle of the detonation waves (or shock waves) reaches a critical value (φ_{cr}), Mach reflection occurs at the position on the central axis from the upper end face, as expressed by the formula $h_c = Lg \cdot tan\varphi_{cr}$ at time t. The pressure at the collision point rises abruptly to the maximum pressure with a maximum of the power capacity. The segmentation and lower end face output opens up a new test method for the optimal design of the special-shaped booster explosive.

Keywords: annular booster pellet, power capability, Mach reflection, overdriven detonation, energy convergence, shock to detonation transition

Acronyms and abbreviations

a_t – Coefficient of the area effect
BASD – Booster pellet axial-steel-dent
MASD – Main charge indirect axial-steel-dent
N – Power exportation capability
p_{CJ} – Theoretical detonation pressure [MPa]
p_{max} – Maximum detonation pressure [MPa]
TP – Test point
φ – Incident angle of a detonation wave
φ_{cr} – Critical value of the collision incidence angle of a detonation wave

1 Introduction

One of the ways is to improve the quality of the explosives by means of the improvement of the oxygen balance, introduction of the high energetic metal powder (such as aluminum) and optimization of the grain gradation of the booster particles [1-11], which can improve the initiating ability of the booster. Another way is to improve the effective power capability of the booster by changing the charge structure of the booster pellet [12], which is mainly realized in one of two distinct ways. s. One is to improve the effective charge of the booster pellet, for example by using a pellet with a hemispherical shape [13, 14]. The other method is to convert the divergent potential energy into the effective initiation energy through the energy convergence effect. When the mass of the charge is the same, the more potential energy converged, the higher the effective power capability and the greater the initiation capacity. One potential geometry to achieve this consists of a concave sphere, a conical outside and a concave spherical inside sphere, ring and conical ring [15-18]. It has been shown from a large number of investigations that there is little hope to synthesize explosives containing C, H, O and N elements with low sensitivity but energy higher than CL-20. Therefore, it is imperative to focus on the design of charging mode and develop the booster pellets that can output higher energy.

It has been shown from many experimental results [15-18] that the initiating ability can be significantly improved by the energy convergence effect produced by changing the structure of the booster pellet. Although high speed camera images can be obtained and analyzed through numerical simulation to establish an intuitive understanding of the evolution law, it is limited in the data that can be acquired which greatly hinders the optimization of design for shaped charges. It is very necessary to find a new way to investigate and understand the energy

accumulation process. Therefore, in this work, the energy convergence effect in the central axis of thane annular booster pellet was investigated by using segmentation and lower end surface output.

2 Experiment

2.1 Geometric model

The test points (TPs) on the central axis of the annular booster pellet are shown in Figures 1 and 2.

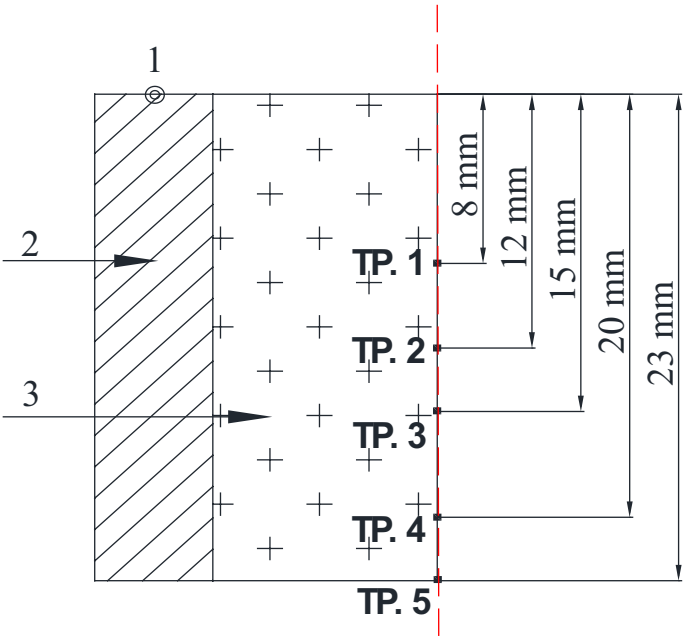

Figure 1. Geometry size of half the axial cross section with TP: 1 – initiating point; 2 – annular booster pellet and 3 – main charge

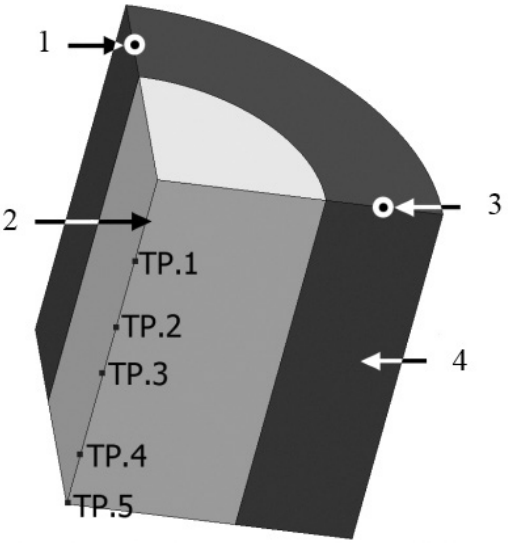

Figure 2. A quarter entities model with TP: 1 – initiating point; 2 – main charge and 3 – annular booster pellet

2.2 Experimental methods

It is difficult to directly measure the output energy on the central axis of an annular booster pellet. Therefore, it is obtained indirectly by using segmentation and using a lower end surface output method, that is, , it is estimated indirectly by examining the energy output from the lower end surface, with the length of the charge being varied to build up a complete picture.

At present, there are many experimental methods to determine the initiation energies of the booster explosive. In this paper, the following two methods are selected [16]:

(i) Booster pellet axial-steel-dent (BASD) method. The booster pellet is in contact with a witness plate, and the booster pellet is detonated with a detonator. The initiation energy is estimated by the axial steel-dent produced by the explosion of the booster pellet.

(ii) Main charge indirect axial-steel-dent (MASD) method. The main charge is detonated directly by the booster charge, and the initiation energy is estimated by the axial steel-dent produced by the explosion of the main charges.

2.3 Experimental condition

The high-energetic explosive PBXN-5, with a density of 1.658 g/cm^3, is used as the booster charge. Five booster pellets of different heights were used (see

Figure 3with corresponding measurements in Table 1). The structures in Figure 1 correspond to those of Figure 3. For example, the length from the vertex to each measuring point in Figure 1 corresponds to the height of each booster in Figure 3, and "TP.1-TP.5" in Figure 1 represents the position of the center point of the lower end surface of each booster in Figure 3. Superfine HMX is used in a four-point-synchronous explosive initiation system and is shown in Figure 4., This initiation system is pressed and formed, with a density of 0.98-1.10 g/cm^3 and the corresponding sizes are in Figure 5 [17].

Figure 3. Annular booster pellets

Table 1. Results of the initiation capacities of annular booster pellets by the BASD and MASD methods

Shape	ρ [g/cm^3]	ϕ_{out} [mm]	ϕ_{in} [mm]	H [mm]	Mass [g]	The dent of BASD method [mm]	The dent of MASD method [mm]	Number of tests
I	1.66	29	19	23	14.40	4.32	0.58	5
II				20	12.50	4.53	0.72	
III				15	9.40	3.58	0.37	
IV				12	7.50	4.24	0.54	
V				8	5.00	3.05	–	

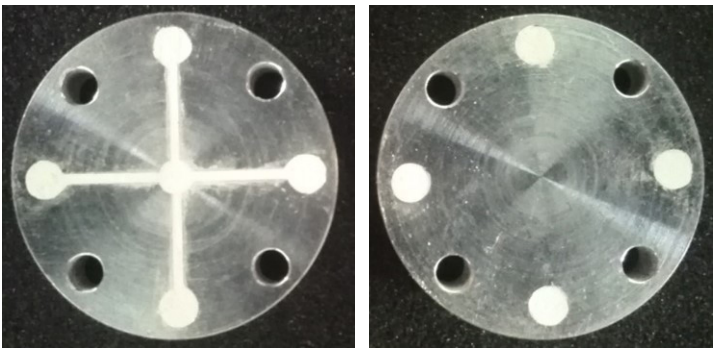

Figure 4. Four-point-synchronous explosive circuit

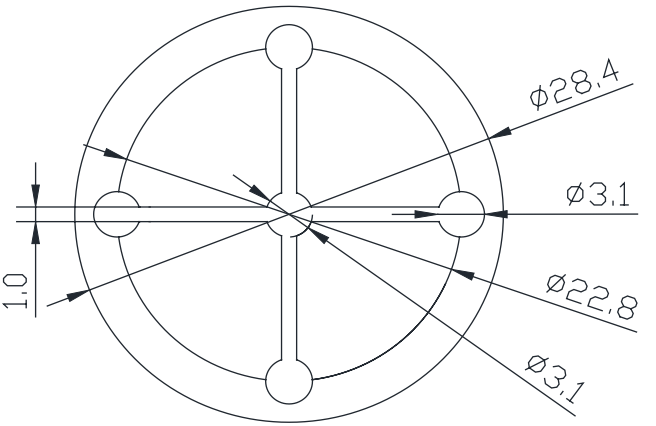

Figure 5. The size of four-point synchronous circuit (in mm)

The components of the main charge include nitroguanidine (NQ), polytetrafluoroethylene (F4) and graphite (G), with the component ratio of NQ/PTFE/G = 51/48/1. Among them, NQ is the explosive component, F4 is the insensitive agent, and G is used as the lubricant and reagent for eliminating the static electricity. The charge density is 1.28 g/cm^3, with a diameter and height of 42.30 and 36.50 mm, respectively. When used with the booster pellets the main charge changes corresponding to the size of the annular booster pellets, so its diameter is 19.00 mm. The material of the witness plate is 45$^{\#}$ steel and the size is 120 (diameter)×50 mm.

2.4 Experimental equipment

The experimental equipment of the initiating ability of the annular booster pellets are shown in Figures 6 and 7.

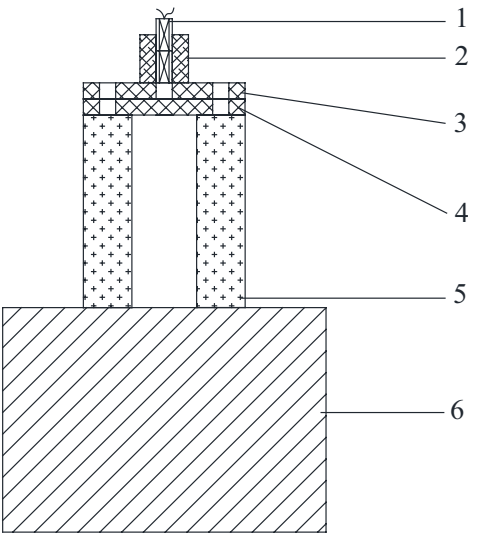

Figure 6. Experimental set-up for BASD method: 1 – detonator, 2 – plastic holder, 3 – circuits cover plate, 4 – circuits substrate, 5 – annular booster pellet and 6 – axial steel witness plate

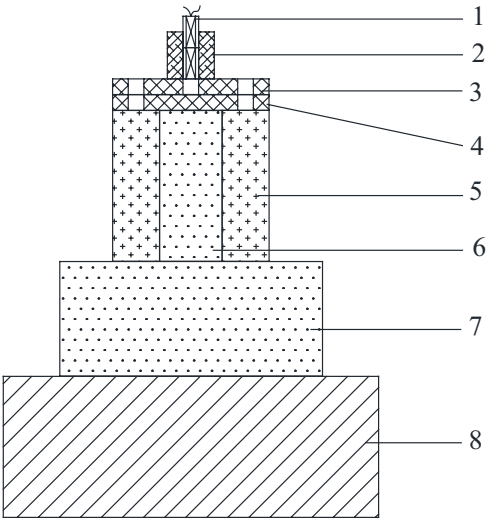

Figure 7. Experimental set-up for MASD method (annular booster pellet under four-point-synchronous explosive circuit): 1 – detonator, 2 – plastic holder, 3 – circuits cover plate, 4 – circuits substrate, 5 – annular booster pellet, 6 – small main charge, 7 – larger main charge and 8 – axial steel witness plate

3 Results

For both BASD and MASD methods, the initiating abilities of the annular booster pellets with the different heights are presented in Figures 8 and 9, and Table 1.

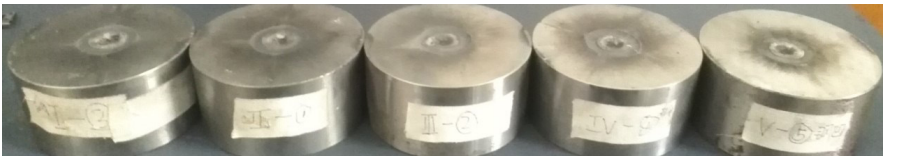

Figure 8. Results of the BASD method

Figure 9. Results of the MASD method

Since the booster charges, main charges and witness plates selected in each of the experiments are similar (see para 2.3) in detail), the influences of the contact surfaces of each other are similar. Therefore, the relationship between the steel dents and heights of the booster pellets in Figure 10 can be approximately transformed into that between the steel dents and depths of the central axis of annular booster pellet after removing the influences of the interfaces by means of moving the same unit vertically up or down, and thus the law will not be changed.

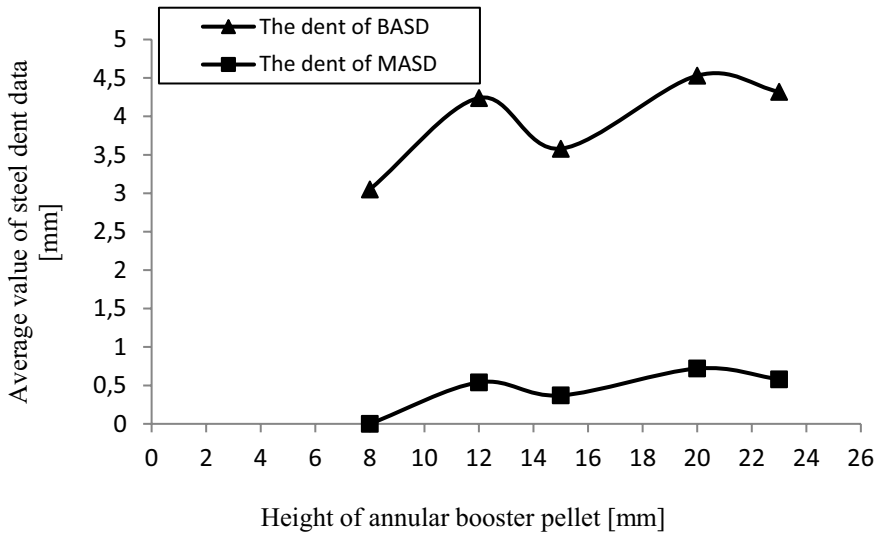

Figure 10. Graph showing the relationship between the dent in steel witness plates and the height of annular booster pellets

4 Discussion

For a traditional cylindrical booster pellet, the value of the maximum detonation pressure (p_{max}) is often equal to or less slightly than the theoretical detonation pressure, according to Chapman-Jouguet conditions, (p_{CJ}) for the given charge density. However, a case of $p_{max} > p_{CJ}$ is often found for the shaped charge structures, such as the annular charge studied here. In the case that the insensitive main charge is detonated by the annular booster pellet, there are two kinds of the detonation waves: one is the annular detonation wave that travels axially down the cyclinder, the other is the convergence effect of the radial detonation wave that travels inwards towards the centre. Among them, the detonation wave convergence from the radial output is dominant.

When the insensitive small main charge inside of the annular booster pellet is detonated by the shock, convergent detonation waves will be generated due to the overdriven detonation from outside to inside of the annular booster pellet [18]. The main characteristic of the convergent detonation waves is that the wavefront of the detonation wave is shrinking, while behind detonation wave is strengthening, and the wave velocity is accelerating, which gradually leads to the overdriven detonation. Thus a pressure will form which is higher than that

from the normal Chapman-Jouguet detonation of the explosive[19, 20]. In the case of a given charge, with the continuous reduction of the distance between the wavefront and axis, the pressure of the convergent detonation waves in the insensitive small main charge increases sharply, and the strongest detonation wave forms at the central axis and propagates downward.

The process of the downward energy flow (shaped energy flow) generated by the convergent detonation waves can be described looking at the wave collision. Compared with the general wave collision, the number of superimposed waves of the convergent detonation waves are more and the abrupt changes of the energies are more significant. According to the collision theory of detonation or shock waves [21, 22]: when two detonation waves (or shock waves) interact head-on, a collision will occur, and the pressure at the collision point increases sharply, as shown in Figure 11. When the incident angle is φ, the detonation waves (or shock waves) will collide obliquely, and two reflected shock waves propagate back to both sides at a certain angle, as shown in Figure 12. For a detonation wave (or shock wave) with a certain Mach number, a normal oblique collision occurs when φ is less than a certain critical angle (φ_{cr}), and the initial incident angle is consistent with the reflection angle, as shown in Figure 13. With the continuous increase of the initial incident angle, the reflection angle of the detonation wave (shock wave) increases. When the incident angle φ reaches φ_{cr}, the incident angle is converted into a "turned incident angle", which forces the reflected shock wave to move up to a certain distance from the collision point, leading to an irregular oblique collision, *i.e.* Mach collision (see Figure 14).

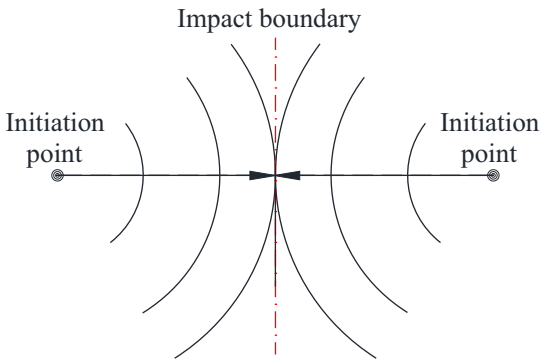

Figure 11. Head-on collision

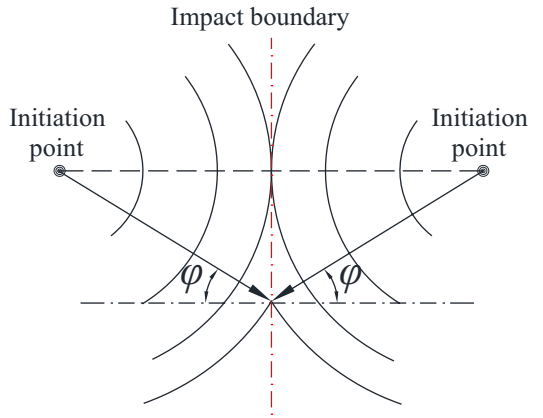

Figure 12. Oblique collision

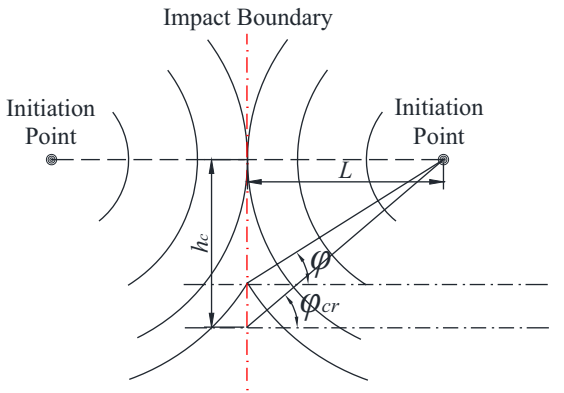

Figure 13. Regular oblique collision ($\varphi < \varphi_{cr}$)

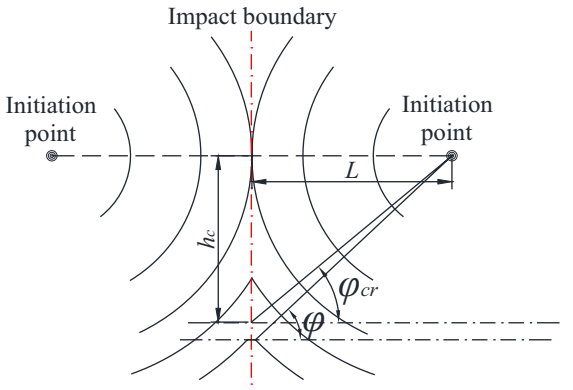

Figure 14. Irregular oblique collision ($\varphi > \varphi_{cr}$)

Here, the formula used to evaluate attenuation pulse power [12] is introduced and adopted to analyses the impact initiation process of the booster (Equation 1).

$$N = \frac{a_t}{Z} \cdot \int_0^{t_c} p^2(t) \cdot dt \tag{1}$$

where N is the power exportation capacity, a_t is the coefficient of the area effect, t is the time, p is the shock pulse pressure, which is a function of the time t, and t_c is the characteristic time for which the shock pulse pressure p decays to the value corresponding to the critical initiation of the sympathetic charge (propellant). Under the given experimental conditions, when the contact areas between the booster and contact material are the same and the materials are the same, the same shock impedances apply. Therefore, it can be concluded that the power exportation capacity N is mainly influenced by the shock pulse pressure p and effective work time t_c.

In the MASD method, the interior of the annular booster is filled with the insensitive small main charge, while as for the BASD method, the interior is only air. At the central axis, when the collision incidence angle of the detonation waves (or shock waves) reaches a critical value φ_{cr}, Mach reflection will occur, and the pressure at the collision point will rise abruptly to a higher value [23]. The position on the central axis can be expressed by Equation 2.

$$h_c = Lg \cdot tan\varphi_{cr} \tag{2}$$

where L is the distance between the initiation point and the frontal collision point, as shown in Figures 13 and 14. Since the shock pressure before Mach reflection is far less than that at the moment of Mach reflection formation, and the action time of the former is less than that of the latter (t_s), there will be a maximum of the power exportation capacity N, which will translate into the pressure much higher than the p_{CJ}, at the moment of the Mach reflection (see Figure 15).

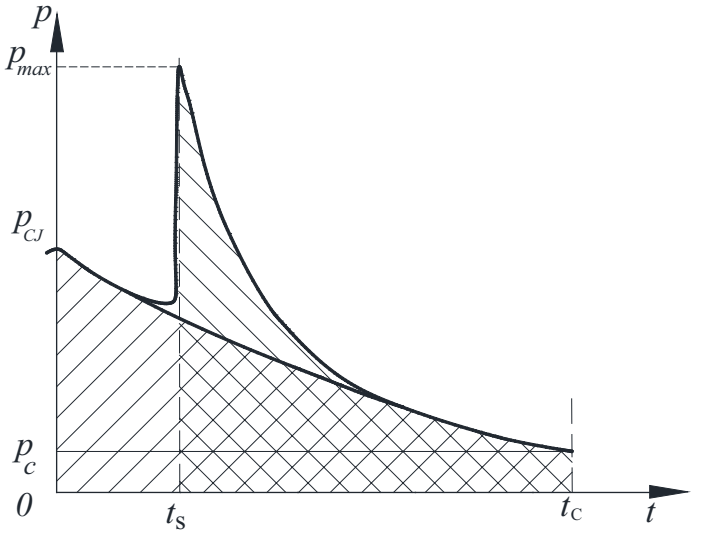

Figure 15. The relation of pressure p and time t in the center axis of annular booster pellet

With the downward movement of the collision point (*i.e.* after Mach reflection), the shock pressure p decreases rapidly [23]. In addition, according to the effective charge theory [24], the action time t increases with the increase of the detonation depth before the charge height reaches the maximum effective charge value. When the initiation detonation occurs in the traditional booster pellet and the detonation pressure reaches p_{CJ}, the power exportation capacity increases gradually with the increase of time t, until it reaches the maximum at the maximum effective time (t_c). Since the converging flow of the energy output along the central axis, plays a dominant role in the shock initiation process (see Figure 15), there must be a maximum value of $\int_0^{t_c} p^2(t) \cdot dt$ with p_{max} corresponding to the time t_s. In other words, in the range of $t_s \sim t_c$, there must be a maximum point, in which N can reach a maximum, as is in agreement with the literature [25]. This proves that the overdriven detonation phenomenon of the shaped charge can be verified indirectly by using the segmentation and lower end face output method.

It is worth mentioning that, the measured results of this experimental method have very high requirements for the synchronization of the detonating explosive network. In general, the initiation capacity of the annular booster pellet could be improved significantly by applying the multipoint synchronous circuit. In order to ensure that the deviation in the intitiation time is as small as possible

it was found that an eight-point synchronous set-up was more effective than the four-point set-up. Due to the difficulty achieving the synchronization of the detonating explosive network, it is difficult to quantify scientifically the trend in evolution of the energy flow in the axis of annular booster pellet. Therefore, in this work, we have only provided the qualitative explanations.

5 Conclusions

For an explosion in air or shock initiation of the insensitive main charge of an annular booster pellet, the evolution laws of the energy convergence effect on the central axis of the internal small main charge (or air) was investigated by using a segmentation and lower end surface output technique. The conclusions are as follows:

- In the process of the annular booster pellet detonated (in air) or shocked to detonation transition, the power capability of the converging energy flow into the central axis increases, then decreases, and then increases and finally decreases.
- When the collision incidence angle of the detonation waves (or shock waves) reaches a critical value φ_{cr}, Mach reflection will occur at the position on the central axis from the upper end face expressed by the formula $h_c = Lg{\cdot}tan\varphi_{cr}$ at time t. The pressure at the collision point will rise abruptly to the maximum pressure in the whole explosion process, and there will be a maximum of the power exportation capacity N.
- Overdriven detonation can be obtained indirectly and conveniently by using the segmentation and lower end face output method, which opens up a new test method for the optimal design of the annular (special-shaped) booster explosive.

Acknowledgements

The authors are grateful for the financial support from by Scientific and Technological Innovation Programs (STIP) of Higher Education Institutions in Shanxi (2020L0639).

References

[1] Xiang, D.-L.; Rong, J.-L.; Li, J.; Feng, X.-J.; Wang, H. Effect of Al/O Ratio on Detonation Performance and Underwater Explosion of RDX-based Aluminized Explosive. (in Chinese) *Acta Armamentarii* **2013**, *34*(1): 45-50; https://doi.org/10.3969/j.issn.1000-1093.2013.01.009.

[2] Davis, J.J.; Miller, P.J. Effect of Metal Particle Size on Blast Performance of RDX-based Explosives. *AIP Conf. Proc.* **2002**, *620*: 950-953; https://doi.org/10.1063/1.1483695.

[3] Woody, D.; Davis, J.J. The Effect of Variation of Aluminum Particle Size and Polymer on the Performance of Explosives. *AIP Conf. Proc.* **2002**, *620*: 942-945; https://doi.org/10.1063/1.1483693.

[4] Tanguay, V.; Goroshin, S.; Higgins, A.J.; Zhang, F. Aluminum Particle Combustion in High-Speed Detonation Products. *Combust. Sci. Technol.* **2009**, *181*(4): 670-693; https://doi.org/10.1080/00102200802643430.

[5] Young, G.; Sullivan, K.; Zachariah, M.R.; Yu, K. Combustion Characteristics of Boron Nanoparticles. *Combust. Flame* **2009**, *156*(2): 322-333; https://doi.org/10.1016/j.combustflame.2008.10.007.

[6] Sullivan, K.; Young, G.; Zachariah, M.R. Enhanced Reactivity of nano-B/Al/CuO MIC's. *Combust. Flame* **2009**, *156*(2): 302-309; https://doi.org/10.1016/j.combustflame.2008.09.011.

[7] Komarov, V.F.; Sakovich, G.V.; Vorozhtsov, A.B.; Vakutin, A.G.; Komarova, M.V. The Function of Nanometals in Enhancing the Explosion Performance of Composite Explosives. *Proc. 40th Int. Annu. Conf. ICT*, Karlsruhe, Germany, **2009**, P108/1-8.

[8] Han, Y.; Huang, H.; Huang, Y.M. Power of Aluminized Explosives with Different Diameters. (in Chinese) *Chin. J. Explos. Propellants* **2008**, *31*(6): 5-7.

[9] Makhov, M. Explosion Heat of Boron-Containing Explosive Compositions. *Proc. 35th* Int. Annu. Conf. ICT, Karlsruhe, Germany, **1999**, P55.

[10] Flower, P.Q.; Steward, P.A.; Bates, L.R.; Shakesheff, A.J.; Reip, P.W. Improving the Efficiency of Metallised Explosives. *Proc. Insensitive Munitions and Energetic Materials Technical Symp.*, Bristol, UK, **2006**.

[11] Wang, C.L.; Zhao, S.X.; Jia, M. Calculation of Detonation Products for Non-ideal Explosive with AP. (in Chinese) *Chin. J. Explos. Propellants* **2014**, *22*(2): 235-239.

[12] Hu, L.S.; Hu, S.Q.; Cao, X. Study on the Initiation Capacities of Two Booster Pellets. *Cent. Eur. J. Energ. Mater.* **2012**, *9*(3): 261-272.

[13] Francois, G.E.; Harry, H.H.; Hartline, L.E.; Hooks, D.E.; Johnson, C.E.; Morris, J.S.; Novak, A.M.; Ramos, K.J.; Sanders, V.E.; Scovel, C.A.; Lorenz, T.; Wright, M.; Botcher, T.; Marx, E.; Gibson, K. *Summary of Booster Development and Qualification Report.* LANL, Report No. LA-UR-12-22394, US, **2012**.

[14] Kong, Q.-Q.; Xu, B.-Y.; Zhong, K.; Lu, Y.-Z. Simulation on the Dynamic Response of Main Charge around the Booster Charge Structure in Penetrating Projectile. (in Chinese) *Initiators Pyrotech.* **2012**, *1*: 1-3.

[15] Hu, S.Q.; Cao, X. A Study on the Structure of Booster Pellets Having High Initiating Capacity. (in Chinese) *Acta Armamentarii* **2002**, *23*(2): 188-190.
[16] Cao, X.; Liu, Y.; Hu, S.Q.; Zhang, S.-Z. Numerical Simulation and Power Test on the Annular Booster Initiated by Multi-point Explosive Circuit. *Initiators Pyrotech.* **2005**, *5*: 16-18+38.
[17] Hu, S.Q.; Liu, H.R.; Hu, L.S.; Cao, X.; Mi, X.-C.; Zhao, H.-X. Study on the Structures of Two Booster Pellets Having High Initiation Capacity. *J. Energ. Mater.* **2014**, *32*(sup1): S3-S12; https://doi.org/10.1080/07370652.2013.812161.
[18] Li, W.X. *One-dimensional Unsteady Flows and Shock Waves*. National Defence Industry Press, Beijing, China, **2003**.
[19] Baker, E.L. *An Explosives Products Thermodynamic Equation of State Appropriate for Material Acceleration and Overdriven Detonation: Theoretical Background and Formulation.* U.S. Army Armament Research, Development and Engineering Center, Technical Report ARAED-TR-91013, NJ, **1991**.
[20] Fritz, J.N.; Hixson, R.S.; Shaw, M.S.; Morris, C.E.; McQueen, R.G. Overdriven-detonation and Sound-speed Measurements in PBX-9501 and the Thermodynamic Chapman-Jouguet Pressure. *J. Appl. Phys.* **1996**, *80*(11): 6129-6141; https://doi.org/10.1063/1.363681.
[21] Zhang, S.Z. *Explosion and Impact Dynamics.* Weapons Industry Press, Beijing, **1993**, pp. 69-83.
[22] Zhang, B.P.; Zhang, Q.M.; Huang, F.L. *Detonation Physics.* Beijing: Weapons Industry Press, China, **2009**, pp. 51-85
[23] Liu, Z.Y. *Overdriven Detonation Phenomenon and Its Application to Ultra-high Pressure Generation.* Kumamoto University, Japan, **2001**.
[24] Huang, Y.S. *Explosive Theory*. Weapons Industry Press, Beijing, **2009**, pp. 202-205.
[25] Xie, Z.B.; Hu, S.Q.; Hu, L.S.; Sun, B.F. Optimal Design of Annular Booster Pellet. (in Chinese) *J. North Univ. China, Nat. Sci. Ed.* **2016**, *37*(2): 177-180+186.

Received: May 12, 2021
Revised: June 26, 2023
First published online: September 28, 2023